Cancer Immunology, Immunotherapy (2021) 70:365–376
https://doi.org/10.1007/s00262-020-02679-5

ORIGINAL ARTICLE

Tumor-selective blockade of CD47 signaling with a CD47/PD-L1 bispecific antibody for enhanced anti-tumor activity and limited toxicity

Yan Wang[1,2,3] · Haiqing Ni[4] · Shuaixiang Zhou[4] · Kaijie He[4] · Yarong Gao[4] · Weiwei Wu[4] · Min Wu[4] · Zhihai Wu[4] · Xuan Qiu[4] · Ying Zhou[4] · Bingliang Chen[4] · Donghui Pan[2] · Chenrong Huang[1,3] · Mingzhu Li[2] · Yicong Bian[1,3] · Min Yang[2] · Liyan Miao[1,3] · Junjian Liu[4]

Received: 12 April 2020 / Accepted: 20 July 2020 / Published online: 6 August 2020

Abstract

CD47, an immune checkpoint receptor frequently unregulated in various blood and solid tumors, interacts with ligand SIPRα on innate immune cells, and conveys a "do not eat me" signal to inhibit macrophage-mediated tumor phagocytosis. This makes CD47 a valuable target for cancer immunotherapy. However, the therapeutic utility of CD47-SIRPα blockade monoclonal antibodies is largely compromised due to significant red blood cell (RBCs) toxicities and fast target-mediated clearance as a result of extensive expression of CD47 on normal cells. To overcome these limitations and further improve therapeutic efficacy, we designed IBI322, a CD47/PD-L1 bispecific antibody which attenuated CD47 activity in monovalent binding and blocked PD-L1 activity in bivalent binding. IBI322 selectively bound to CD47+PD-L1+ tumor cells, effectively inhibited CD47-SIRPα signal and triggered strong tumor cell phagocytosis in vitro, but only with minimal impact on CD47 single positive cells such as human RBCs. In addition, as a dual blocker of innate and adaptive immune checkpoints, IBI322 effectively accumulated in PD-L1-positive tumors and demonstrated synergistic activity in inducing complete tumor regression in vivo. Furthermore, IBI322 showed only marginal RBCs depletion and was well tolerated in non-human primates (NHP) after repeated weekly injections, suggesting a sufficient therapeutic window in future clinical development of IBI322 for cancer treatment.

Keywords Immunotherapy · Adaptive immunity · Phagocytosis · Innate immunity · Bispecific antibody · IBI322

Abbreviations

ATCC	American Type Culture Collection
DCs	Dendritic cells
DFO	P-SCN-Deferoxamine
IBI322	An anti-CD47/PD-L1 bispecific antibody
NHPs	Non-human primates

Electronic supplementary material The online version of this article (https://doi.org/10.1007/s00262-020-02679-5) contains supplementary material, which is available to authorized users.

Yan Wang, Haiqing Ni and Shuaixiang Zhou contributed equally to this work.

✉ Min Yang
yangmin@jsinm.org

✉ Liyan Miao
miaolysuzhou@163.com

✉ Junjian Liu
junjian.liu@innoventbio.com

[1] Department of Clinical Pharmacology, First Affiliated Hospital of Soochow University, 899 Pinghai Road, Gusu District, Suzhou 215006, Jiangsu Province, China

[2] NHC Key Laboratory of Nuclear Medicine, Jiangsu Key Laboratory of Molecular Nuclear Medicine, Jiangsu Institute of Nuclear Medicine, 20 Qianrong Road, Binhu District, Wuxi 214063, Jiangsu Province, China

[3] Institute for Interdisciplinary Drug Research and Translational Sciences, College of Pharmaceutical Sciences, Soochow University, Suzhou, China

[4] Innovent Biologics (Suzhou) Co., Ltd., 168 Dongping Street, Suzhou Industrial Park, Suzhou 215123, Jiangsu Province, China

PD-L1 Programmed death-ligand 1
PD-1 Programmed death-1
RBCs Red blood cells
SIRPα Signal-regulatory protein-α

Introduction

Functioning as an innate checkpoint molecule, CD47, a ligand of signal-regulatory protein-α (SIRPα), transmits an inhibitory signal to calreticulin-activated phagocytosis in macrophages [1, 2]. The CD47/SIRPα pathway has been recognized as a critical mechanism through which cancer cells evade innate immune surveillance [3, 4]. CD47 is frequently overexpressed in various hematological malignancies and solid tumors. High CD47 levels were strongly associated with poor prognosis in patients [3]. Agents that block CD47/SIRPα interactions have demonstrated significant anti-tumor activities as a monotherapy or in combination with tumor targeting antibodies in multiple preclinical tumor models [3–6]. Promising clinical efficacies had been observed in relapsed/refractory non-Hodgkin's lymphoma patients treated with anti-CD47 mAb Hu5F9 in combination with rituximab [5, 7]. A decent objective response rate has also been reported in acute myeloid leukemia (AML) patients treated with Hu5F9 [8]. However, the therapeutic utility of CD47 blockade antibodies has been hampered by suboptimal pharmacokinetic properties and tolerability issues [9]. On one hand, ubiquitous expression of CD47 in human body results in an "antigen sink" effect, which requires frequent administration of high-dose CD47 to achieve sufficient drug exposure in patients. On the other hand, high exposure of CD47 antibody induces more target-related adverse events such as anemia [7]. Moreover, although remarkable anti-tumor efficacy has been demonstrated in multiple preclinical models, CD47 blocking agents have so far only exhibited modest efficacy in patients with solid tumors [9]. It is conceivable that, in complex immunosuppressive microenvironment of heterogeneous tumors, cancer cells may adopt multiple mechanisms to escape immune surveillance. Thus activating innate immunity alone may be insufficient to eradicate malignant cells. Alternatively, harnessing both innate and adaptive immune responses may present a more effective strategy to induce durable anti-tumor activity [10–12].

PD-L1 is an inhibitory membrane protein overexpressed in tumor cells and regulatory immune cells in the tumor microenvironment [13]. After binding to its receptor PD-1, PD-L1 suppresses tumor-specific T cell functions to create a locally deficient immune environment and prevent T cell-mediated tumor eradication [14]. Significant objective responses have been achieved by anti-PD-1 therapies in a broad spectrum of tumors with tolerable immune-related adverse events in patients. Currently, at least six anti-PD-1/PD-L1 products have been approved by the FDA for various indications [15–18]. Studies have elucidated a novel role of PD-1 in tumor-associated macrophages (TAMs). PD-1 expression on M2 macrophages has been linked with decreased phagocytotic activity. Blockade of PD-1/PD-L1 signaling has been shown to restore TAM phagocytosis and synergize with CD47 antibody in reducing tumor growth in macrophage-dependent mechanisms [19]. This underscores the direct effect of anti-PD-1 therapies in regulating innate immunity. In syngeneic models, CD47 blockade triggers a strong anti-tumor T cell response to destruct established tumors, indicating the critical role of CD47 in bridging innate DC and adaptive T cell immunity [19]. These studies have provided a strong scientific rationale to simultaneously target CD47/SIRPα and PD-1/PD-L1 pathways for optimal immune activation and effective tumor destruction [19].

Herein, we describe IBI322, a novel, "1 + 2" CD47/PD-L1 dual-targeting bispecific antibody. By an "imbalanced" design with lower binding affinity to CD47 versus higher binding to PD-L1, the molecule is expected to block CD47 on CD47+/PD-L1+ tumors in a more selective manner than a regular CD47 monoclonal antibody does. Furthermore, we are very interested to investigate the potential synergy of activating both innate and adaptive immunity in cancer treatment. This study aims to characterize the mechanism of actions of IBI322 in vitro and in vivo, and to demonstrate its potential in future clinical development.

Material and methods

Cell lines, antibodies, and reagents

All cell lines were purchased from ATCC. MC38-PD-L1-CD47 co-expressed cell line and Raji-PD-L1 (CD47+PD-L1+) overexpressed cell line were generated by lentivirus infection using standard protocols. CHO-S stable cell lines overexpressing human CD47 or PD-L1 were generated using Freedom CHO-S Kit (Invitrogen). Human PD-L1 was inserted into pCHO 1.0 vector (Invitrogen) for the generation of CCRF-CEM cells overexpressing PD-L1. Anti-PD-L1, anti-CD47, and IgG Isotype control were generated at Innovent Biologics (Suzhou) Co., Ltd. Recombinant PD-L1, CD47, SIRP-α murine Fc fusion, and PD-1 murine Fc fusion were acquired from ACROBiosystems.

Bispecific antibody production and characterization

IBI322 was designed in a "1 + 2" format using knobs-into-holes strategy [20]. Antibody was isolated on MabSelect SuRe (GE Healthcare) and then further purified by Mono S chromatography (GE Healthcare) according to the manufacturer's protocols. The purity and molecular weight of

IBI322 were analyzed by analytic size exclusion chromatography (SEC) and mass spectrometry (Agilent Technologies), respectively. Affinity was determined by bio-layer interferometry (BLI)-based Octet RED96 (Pall ForteBio). PD-L1 and CD47 were biotinylated with EZ-Link Sulfo-NHS-LC-Biotin kit (Thermo Fisher Scientific), and loaded onto SA–streptavidin biosensors (Pall ForteBio) at 150 μg/mL. After washing, sensors were dipped into buffer containing antigen then dissociated in sample dilution buffer (50 mL PBS + 0.1% BSA + 0.05% Tween-20). Data analysis was carried out using ForteBio software.

Cell-based binding and blocking assay

CHO-hPD-L1 cells or RBCs were incubated with antibodies for 30 min in PBS, followed by three washes and subsequent incubation with a secondary antibody PE-anti-human IgG (Southern Biotech) for 30 min. For CD47 blocking experiments, antibody was added in the presence of hSIRPα-mFc protein. The mixture was incubated with CHO-hCD47 cells or CCRF-CEM-PD-L1 cells (0.2×10^6 cells/well) for 30 min. For PD-L1 blocking assay, antibody was added in the presence of human PD-1-mFc protein. Then, the mixture was incubated with CHO-hPD-L1 cells (0.2×10^6 cells/well) for 30 min, followed by three washes and subsequent incubation with a secondary antibody APC goat anti-mouse IgG (BioLegend) in PBS for 30 min. Flow cytometry was performed on a FACSCELESTA (BD Biosciences) and MFI was calculated accordingly.

In vitro phagocytosis assay

CD14 + monocytes were isolated from fresh human peripheral blood mononuclear cells (PBMCs) and then induced to differentiate into macrophages by incubating with GM-CSF (10 ng/mL) for 7 days. On day 5, interferon gamma (IFNγ; 20 ng/mL) was added to stimulate for 1 h, followed by lipopolysaccharide (LPS) for 48 h (100 ng/mL). CFSE-labeled (Thermo Fisher Scientific) CCRF-CEM-PD-L1 tumor cells were incubated with human macrophages (ratio 4:1) with antibody at 37 °C for 3 h. Cells were washed three times with PBS, and incubated with APC mouse anti-human CD14 antibody (BD Biosciences) for 30 min. Phagocytosis was measured by assessing the percentage of CFSE + cells in CD14 + cells via flow cytometry.

Mixed lymphocyte reactions (MLR)

CD4+ T cells were isolated from human PBMC (AllCells) using EasySep human CD4+ T cells enrichment kit (StemCell Technologies). DCs were generated by incubating PBMC first with IL-4 (20 ng/mL) and GM-CSF (10 ng/mL) for 5 days, followed by maturation in media-containing tumor necrosis factor (10 ng/mL), IL-1β (5 ng/mL), IL-6 (10 ng/mL), and prostaglandin E2 (1 μM) for 2 days. 1×10^4 DCs and 1×10^5 CD4 + T cells were seeded in X-VIVO-15 medium and incubated with antibody. IFNγ level in culture supernatants was measured 3 days later.

In vitro selective binding assay

H292 cells (CD47+/PD-L1+ tumor cells) were labeled with CFSE and mixed with 20-fold human RBCs. Cell mixtures were incubated with antibody at different concentrations for 30 min in PBS on ice. Then, cells were washed with PBS three times, followed by incubation with a secondary antibody APC anti-human IgG (BioLegend) in PBS for 30 min on ice. Cells were washed at least twice with PBS and analyzed with flow cytometry.

In vitro selective phagocytosis assay

RBCs were separated from a healthy human donor's blood sample with Ficoll (StemCell Technologies) according to the manual. For macrophages, bone marrow from NOD-SCID mice was isolated and cultured in M-CSF for 6 days. Thereafter, macrophages were stimulated with LPS for 16–24 h before use. Cell track green (CMFDA), red (CMPTX), and violet (CMF2HC) labeled Raji-PD-L1 was mixed with RBCs at a 1:500 ratio. The cell mixture was stained with human IgG (h-IgG), anti-CD47 antibody, or IBI322 bispecific antibody to occupy CD47 on tumor cell surface. Then, tumor cells were co-cultured with activated macrophages at 37 °C in a humidified atmosphere containing 5% CO_2 after lysis of RBCs in the cell mixture. Images were recorded every 5 min for 6 h using imaging station CellR (Olympus Corporation).

In vivo model

For Raji-PD-L1 model, each NOD-SCID mouse (Beijing Vital River Laboratory) was intravenously injected 1×10^6 human PBMC 6 days before Raji-PDL1 cell implantation (9×10^6 cells/mouse) at the right back. 5 days after tumor implantation, 40 mice with tumors were randomized into five treatment groups.

For A375 model, each NOG mouse (Beijing Vital River Laboratory) was intravenously injected 2×10^6 human PBMC 6 days before A375 implantation (6×10^6 cells/mouse) at the right back using a method previously reported [21]. 2 days after tumor implantation, 40 mice with tumors were randomized into five treatment groups.

Drugs were intraperitoneally injected once every 2 days for six continuous doses. Body weight, maximum length of major axis (L), and maximum length of minor axis (W)

of tumors were measured twice a week for 29 days. Tumor growth inhibition (TGI) of each mouse was calculated.

Biodistribution

Three antibodies (IBI322, αCD47 and αPD-L1) were conjugated with p-SCN-Deferoxamine (DFO; Macrocyclics), then radiolabeled with ^{89}Zr (Perkin Elmer, Inc.) using a method previously reported [22, 23]. 18 huCD47 knock-in mice (Biocytogen, Inc.) bearing MC38 tumor (transfected huCD47 and huPDL1) were used to investigate tumor uptake and organ distribution. They were randomized into five groups according to tumor volume (100–250 mm^3): ^{89}Zr-Df-IBI322 group ($n=4$, 3.39 ± 0.10 MBq, 0.50 ± 0.02 mg/kg), equimolar ^{89}Zr-Df-αCD47 ($n=4$, 3.12 ± 0.18 MBq, 0.51 ± 0.03 mg/kg), ^{89}Zr-Df-αPD-L1 (n = 4, 3.53 ± 0.25 MBq, 0.32 ± 0.03 mg/kg), as well as two control groups: ^{89}Zr-oxalate ($n=3$, 3.26 ± 0.11 MBq) and ^{89}Zr-DFO ($n=3$, 1.46 ± 0.10 MBq). PET images were acquired at 2, 24, 48, 72, 120, and 168 h after injection of the radiotracer. Quantification of PET images was accomplished in an Inveon Research Workplace ASIpro (Siemens Healthineers) workstation via region of interest (ROIs) or volume of interest (VOI s, for tumor only) analysis; tissue uptake values were reported as percent injected dose per gram of tissue (%ID/g).

NHP study

An NHP study was conducted at JOINN Laboratories (Suzhou, China) in accordance with standard operating procedures. Experimentally non-naive, socially housed cynomolgus monkeys ($n=3$/group, 2.5–5 years of age and weighing 2.51–2.84 kg at the onset of the day) were administered mAbs on days 1, 8, and 15 by IV injection with IBI322 or anti-CD47 mAb Hu5F9 at dosing of 10 mg/kg. Animals were observed at least twice daily. Peripheral blood was collected for hematology assessment and clinical pathology evaluation.

Statistical analysis

Results are presented as mean ± SEM. Statistical analyses were carried out using Prism 8.0 statistical software (GraphPad Software Inc.). Statistical significance for tumor volume between groups was determined by one-way ANOVA, and p values of less than 0.05 were considered to be statistically significant. Asterisks indicate statistical compared to h-IgG group unless otherwise indicated in the figures ($^*p<0.05$, $^{**}p<0.01$, $^{***}p<0.001$, and $^{****}p<0.0001$).

Results

Generation and characterization of IBI322

IBI322 was generated in a "1 + 2" format using knobs-into-holes strategy [20] (Fig. 1a). The anti-CD47 arm (ADI29341; knob) is in Fab format, and the anti-PD-L1 arm (bi127; hole) consists of two single domain antibodies (VHH) in tandem with an amino acid linker (4*GGGGS). IBI322 was stably expressed by CHO cells, captured on protein A resin and then polished from antibody fragments by cation exchange chromatography (CEX). The result of SEC purity showed a very low level of aggregation (Fig. 1b, < 0.9%,) and LC–MS analysis showed a main mass deconvolution peak corresponding to the expected heterodimer with an absence of significant amounts of either homodimer (Supplementary Fig. S1).

To confirm the binding activity of IBI322 to each antigen, CD47/PD-L1 binding activity of IBI322 was evaluated by BLI. As shown in Fig. 1c and d, K_D of IBI322 was determined to be 0.07 nM for hPD-L1 and 1.11 nM for hCD47, showing similar potent binding affinities as the parental antibodies (Supplementary Fig. S2). The high-affinity 2-VHH anti-PD-L1 arm serves to tether the antibody to PD-L1/CD47 double-positive cells. In binding to CD47 on RBCs, IBI322 showed a much lower affinity (2.428 nM) than the parental anti-CD47 (0.1759 nM) (Fig. 1e). This suggest that, with a weak monovalent CD47 binding arm, IBI322 binds to CD47 single positive cells less potently than bivalent parental anti-CD47 antibody. Cell-based binding experiments on CHO cells overexpressing human PD-L1 (CHOS-PD-L1) were investigated by flow cytometry. The EC_{50} value was 1.421 nM, which was similar to the parental anti-PD-L1 antibody (Fig. 1f).

IBI322 enhanced human T cell activation and promoted human macrophage phagocytosis in vitro

In this study, the blocking activity of IBI322 on PD-1/PD-L1 and CD47/SIRPα interaction was investigated. IBI322 efficiently inhibited PD-1 binding to PD-L1 on CHOS-PD-L1 cells (CHOS-PD-L1) with IC_{50} at 1.712 nM, similar to the parental anti-PD-L1 (Supplementary Fig. S3A). However the blocking activity of IBI322 on CD47/SIRPα interaction was 30-fold lower than the parental anti-CD47 on CD47+CHOS cell (Fig. 2a). Interestingly, the blocking activity of IBI322 on CD47/SIRPα interaction was restored on PD-L1+CD47+ human tumor cell CCRF-CEM-PD-L1 (Fig. 2b). These results confirmed that PD-L1 co-engagement enhanced CD47 blockade at the surface of CCRF-CEM-PD-L1 tumor cells.

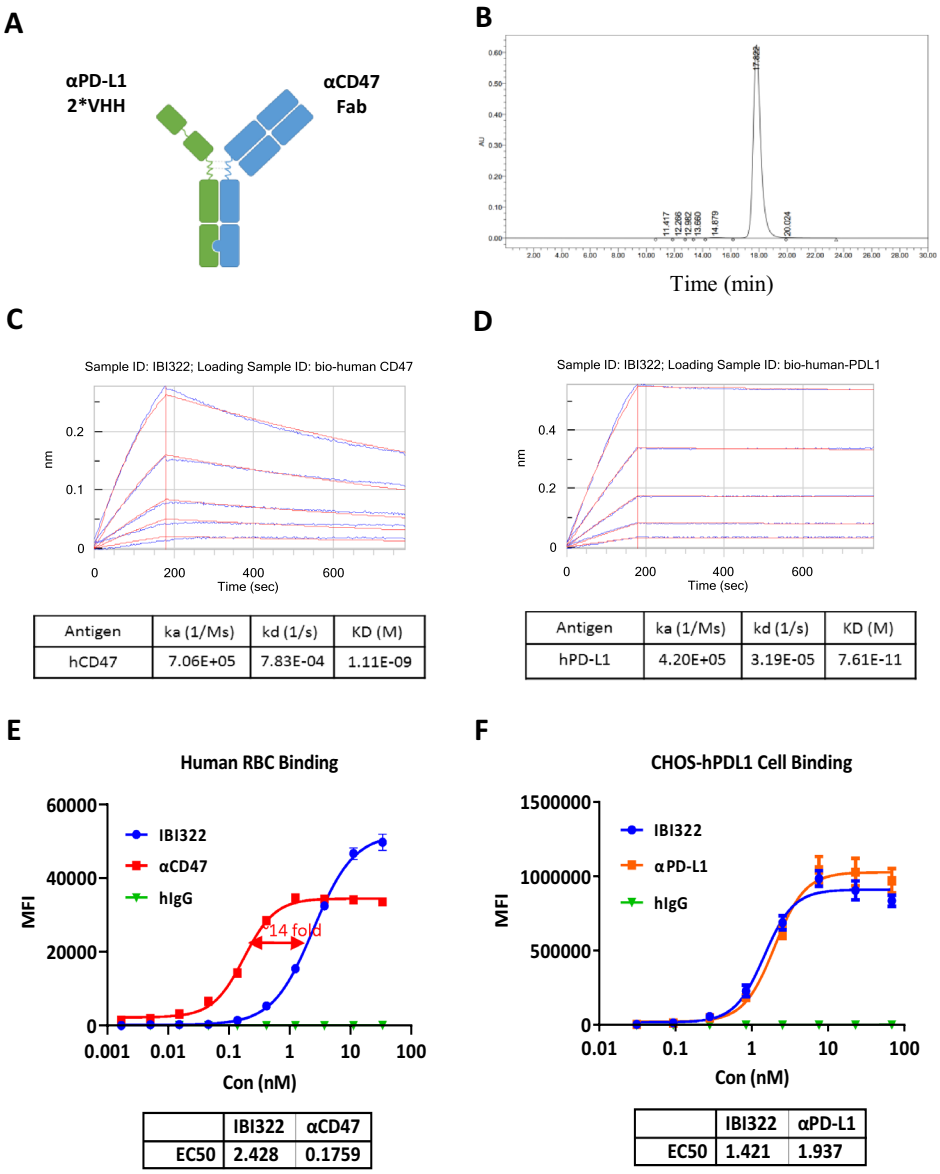

Fig. 1 Design and characterization of IBI322. **a** The schematic diagram of IBI322. **b** SEC-HPLC purity of IBI322 after two-step purification. **c**, **d** Association and dissociation of IBI322 to hPD-L1 and hCD47. **e** Affinity of IBI322 to RBCs. **f** Affinity of IBI322 to CHO-hPD-L1 cells

The T cell activation of IBI322 was also investigated with an MLR assay. In the experiment, IBI322 significantly increased IFNγ levels in a concentration-dependent manner, just like the parental anti-PD-L1 (Supplementary Fig. S3B). Subsequently, IBI322 activity in inducing phagocytosis of macrophages was analyzed. The data demonstrated that, similar to the parental anti-CD47, IBI322 significantly increased phagocytosis of CCRF-CEM-PD-L1 in a concentration-dependent manner (Fig. 2c). These results revealed that IBI322 was effective in promoting phagocytosis of macrophages and stimulating T cell activation in system with dual-antigen expressing tumor cells.

IBI322 selectively targeted CD47/PD-L1 double-positive tumor cells in vitro and induced more potent phagocytosis

Given the broad expression of CD47, a general concern for systemic administration of current CD47 targeting reagents is off-tumor/on-targeting toxicity, which results in impaired therapeutic efficiency and significant side effects. A major reason for the design of IBI322 is to achieve the therapeutic benefit of selectively blocking CD47-SIRPα interaction on PD-L1+CD47+ tumor cells, while avoiding a potential "antigen sink" created by CD47 molecules on RBCs and other normal cells. To determine the selective binding of IBI322 to double-positive tumor cells in the presence of excess CD47+RBCs, PD-L1+CD47+H292

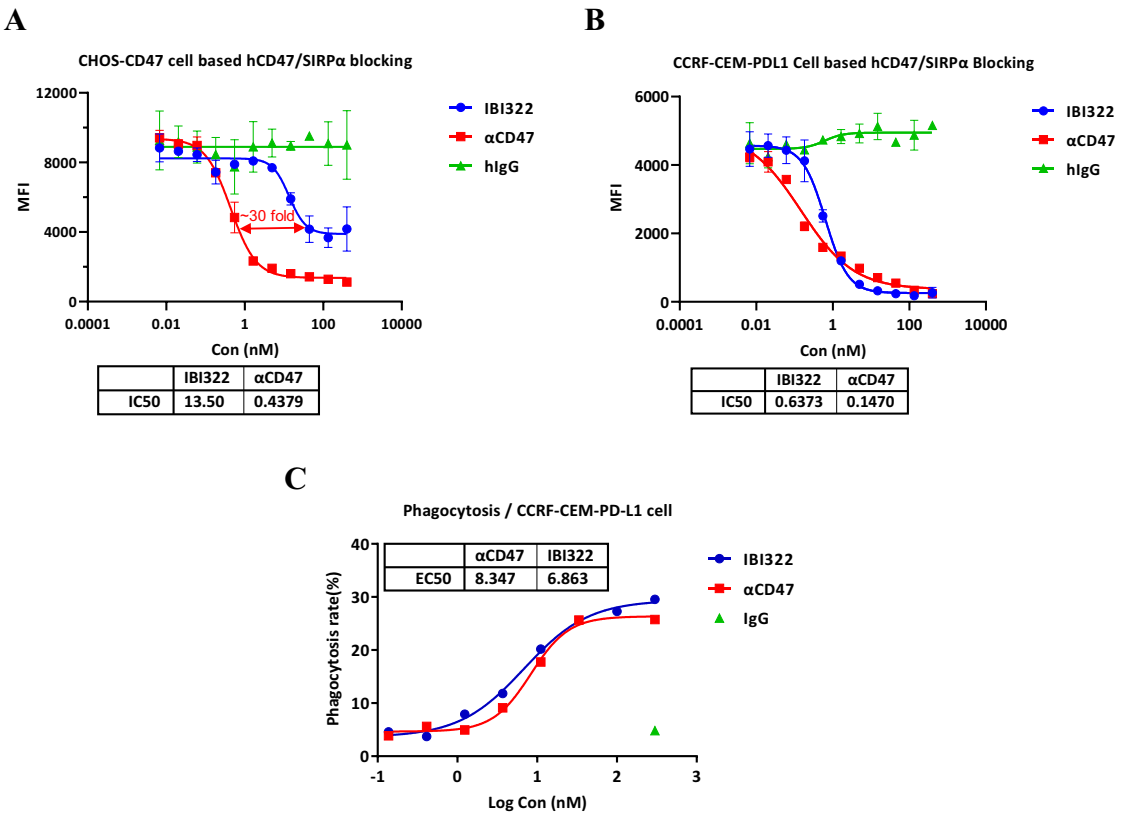

Fig. 2 IBI322 promotes human macrophage phagocytosis. **a** IBI322 partly blocks the hCD47/SIRPα signaling in CHOs-CD47 cells. **b** IBI322 potently blocks hCD47/SIRPα signaling in PD-L1 + CD47 + tumor cells. **c** IBI322-mediated phagocytosis of CCRF-CEM-PD-L1 cells

tumor cells were labeled with CFSE and mixed with a 20-fold excess of unlabeled RBCs, then incubated with antibodies (Fig. 3a). Similar to the parental anti-PD-L1antibody, after incubation with IBI322, the majority of cells bound by antibody were double-positive H292 cells, and only few cells were RBCs (Fig. 3b, c). In contrast, after incubation with the parental anti-CD47, majority of cells bound by anti-CD47 were RBCs (Fig. 3b, c). These results suggested that IBI322 selectively bind to PD-L1+CD47+tumor cells, even in the presence of RBCs.

Furthermore, to visualize and confirm phagocytic activity of macrophages in the presence of IBI322-opsonized tumor cells, live imaging was performed. In this study, the same tumor cell lines, PD-L1+CD47+Raji cells, were CMFDA-labeled (green), CMPTX-labeled (red), and CMF2HC-labeled (violet) separately in the presence of excess CD47+RBCs (1:500), then incubated with anti-CD47, IBI322, or irrelevant human IgG, and further mixed together and cultivated along with macrophages (Fig. 4a). Figure 4b clearly showed that tumor cells are indeed engulfed by macrophages and not just attached to their membranes. Moreover, and as expected, PD-L1+CD47+Raji cells pre-incubated with IBI322 are phagocytosed efficiently while anti-CD47 mono induced weak phagocytosis, which was inhibited by RBCs due to RBC selective binding (Fig. 4c). No phagocytosis was seen when using an irrelevant human IgG control antibody (Fig. 4c).

Organ biodistribution in tumor bearing mice

To investigate the distribution characteristics of bispecific antibody IBI322 in vivo, ^{89}Zr labeled antibodies were administered in huCD47 transgenic mice inoculated with MC38-PD-L1-CD47 cells. Then a PET scanning was performed to detect isotope distribution (Fig. 5). As expected, similar to the parental PD-L1 antibody, IBI322 showed significantly higher tumor uptake and lower heart, liver, and spleen uptake than the parental CD47 antibody (Fig. 5a, b, c). In addition, the uptake of anti-CD47 mAb by heart in the first hour was more than 50% higher than that of IBI322, then the uptake of both antibodies gradually declined to similar levels after 7 days. The retention of anti-CD47 mAb in spleen was almost twofold higher than that of IBI322 over a 7-day course (Fig. 5b, c). This data further demonstrated that IBI322 selectively bound to CD47/PD-L1 double-positive

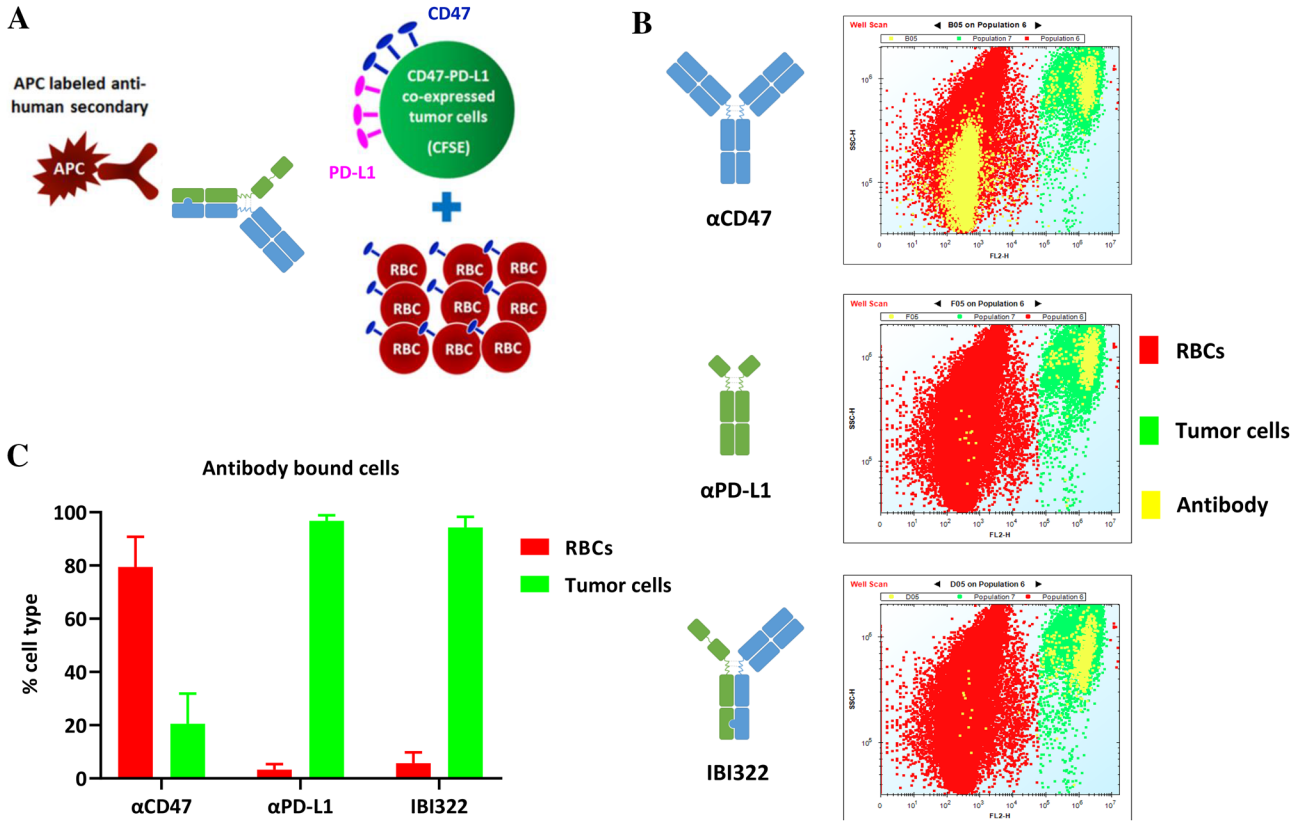

Fig. 3 IBI322 selectively binds to dual antigen-expressing cells in the presence of RBCs. **a** Schematic of the experimental design to assay for selectivity in binding to H292 tumor cells (CD47/PD-L1 double positive cells) in the presence of excessive RBCs (CD47 single positive cells). H292 cells were labeled with CFSE and mixed with a 20-fold excess of RBCs. Cell mixtures were incubated with primary antibody prior to staining with APC anti-human Fc secondary antibody, then analyzed by flow cytometry. **b**, **c** Percentages of H292 tumor cells (CFSE +) and RBCs (CFSE −) within the antibody-bound (APC +) population

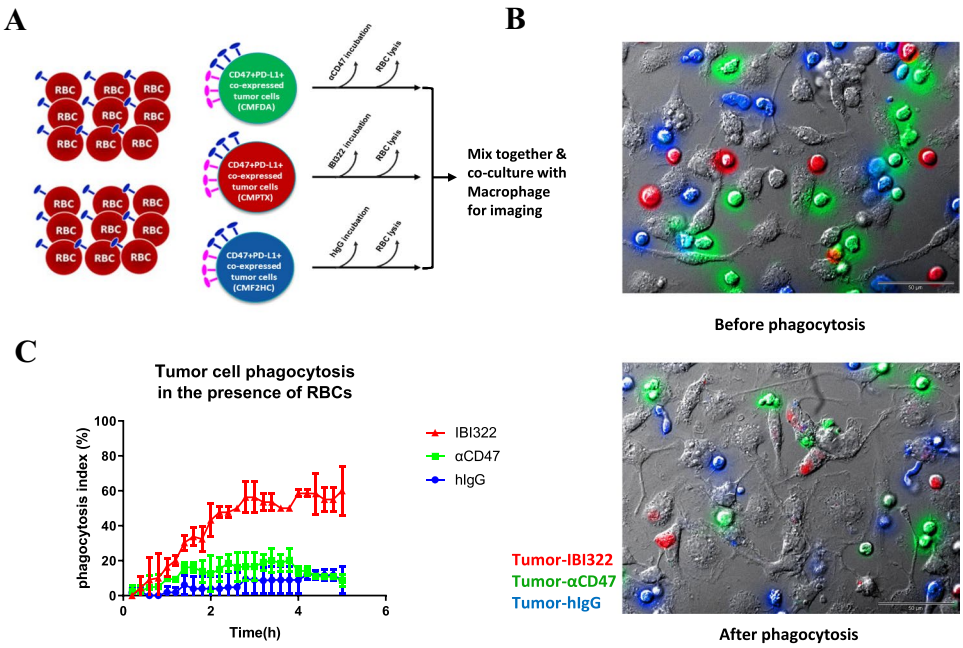

Fig. 4 IBI322 selectively bound to tumor cells to induce more potent phagosytosis. **a** Schematic of the experimental design to assay. Tumor cells treated with IBI322 were labeled with red fluorescence (CMPTX). Tumor cells treated with CD47 were labeled with green fluorescence (CMFDA). Tumor cell treated with h-IgG were labeled with blue fluorescence (CMF2HC). These three cell populations were mixed together and further cultivated together with macrophages. **b**, **c** IBI322 induced potent tumor phagocytosis, but anti-CD47 only caused weak phagocytosis which was inhibited by RBCs due to RBC selective binding

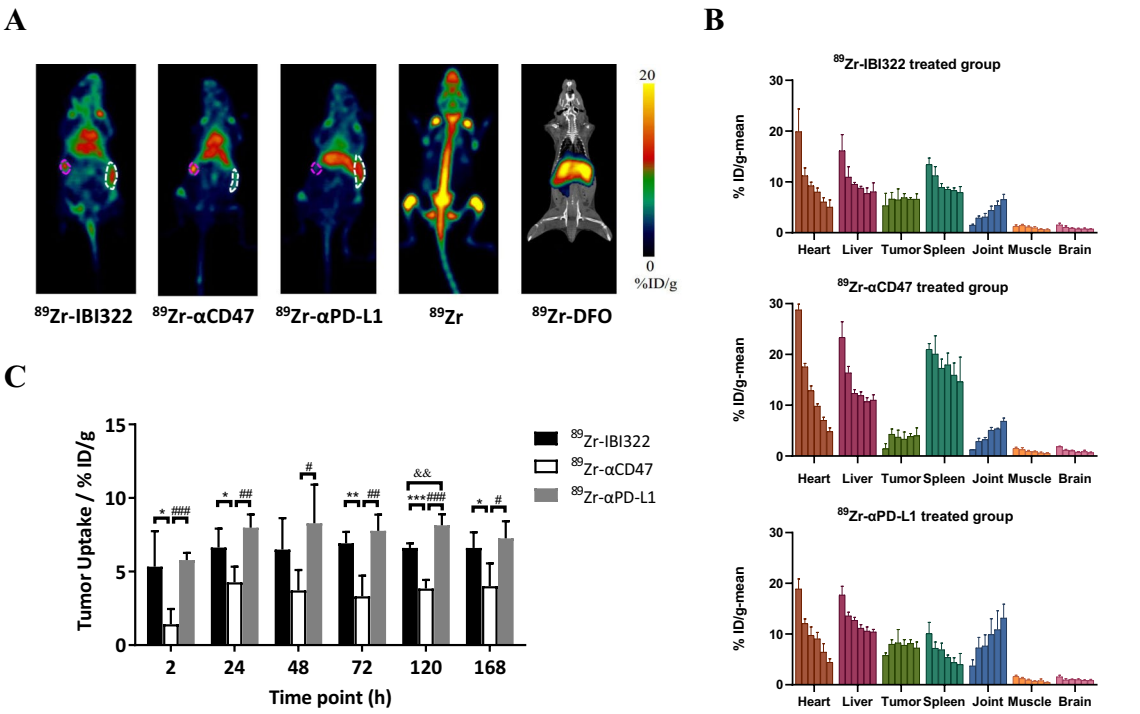

Fig. 5 IBI322 selectively binds to dual antigen-expressing tumor cell PET/CT imaging in tumor-bearing mice. **a**, **b** Compared to anti-CD47, IBI322 showed significantly higher tumor uptake and lower heart, liver, and spleen uptake. Tumor and spleen are indicated by white pink circles, respectively. **c** Time course quantification of tumor uptake treatment with IBI322, anti-PD-L1, and anti-CD47

tumor cells, while with reduced binding activity to normal cells, especially to RBCs.

IBI322 inhibited tumor growth in vivo

To evaluate in vivo anti-tumor activity of IBI322, NOD-SCID mice with PD-L1/CD47-expressing Raji tumor were treated with antibodies. The result is shown in Fig. 6a and S4. All other treatment groups, including anti-CD47

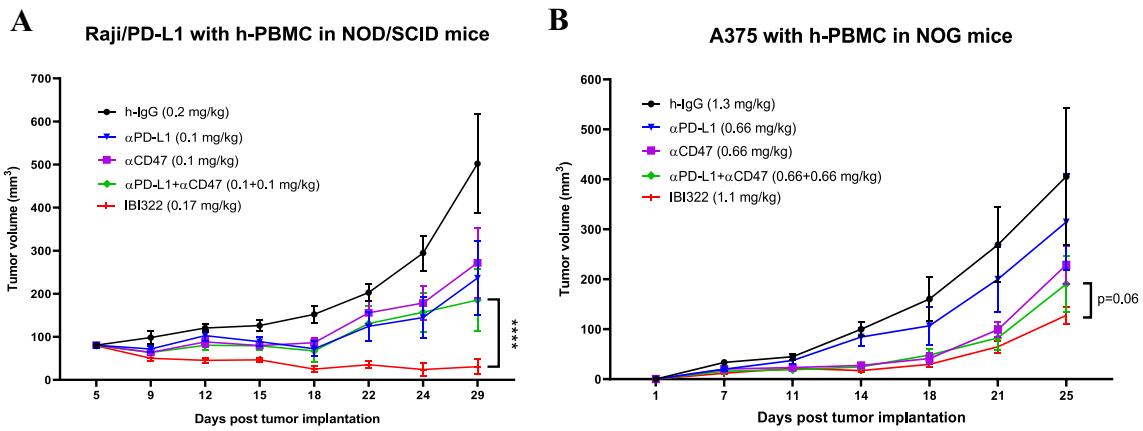

Fig. 6 Superior anti-tumor activity of IBI322 treatment in mouse models reconstituted with human PBMC. **a** Tumor growth of Raji-PDL1 tumor-bearing mice treated with h-IgG 0.20 mg/kg, anti-PD-L1 0.1 mg/kg, anti-CD47 0.1 mg/kg, anti-PD-L1 + anti-CD47 0.1 + 0.1 mg/kg, and IBI322 0.17 mg/kg. **b** Tumor growth of A375 tumor-bearing mice treated h-IgG 1.30 mg/kg, anti-PD-L1 0.66 mg/kg, anti-CD47 0.66 mg/kg, anti-PD-L1 + anti-CD47 0.66 + 0.66 mg/kg, and IBI322 1.1 mg/kg. Tumor growth was measured twice a week and is shown as average tumor size per group ± SEM. Statistical significance was determined by two-way ANOVA

monotherapy, anti-PD-L1 monotherapy, and the combo of anti-PD-L1 and anti-CD47, were effective in delaying Raji tumor progression. It is particularly noteworthy that, on equal molar basis, the treatment with IBI322 resulted in significantly rapid and a nearly complete response at 0.17 mg/kg compared to anti-CD47, anti-PD-L1, as well as the combination of these two antibodies at 0.1 mg/kg each (Fig. 6a). Meanwhile, no abnormal body weight changes or signs of toxicity throughout the study were observed (supplementary Fig. S4).

In A375 xenograft mouse model, the parental anti-PD-L1 antibody treatment at 0.66 mg/kg only showed weak efficacy in delaying tumor progression (Fig. 6b and supplementary Fig.S5). Tumor growth was significantly slower in both the parental ant-CD47 treatment at 0.66 mg/kg and the combination treatment of CD47 and PD-L1 blockade (Fig. 6b). However, most significant tumor regression was observed in IBI322 treatment at 1.1 mg/kg on equal molar basis (Fig. 6b). Meanwhile, no abnormal body weight changes or signs of toxicity throughout the study were observed (supplementary Fig. S5). These results demonstrated IBI322 as a potent treatment in inhibiting tumors growth.

IBI322 had lower risks of hematological toxicities than CD47 mAb in NHPs

A NHP study was conducted to further explore the toxicity profile of IBI322. Cynomolgus monkeys ($N=3$) were treated by IV injection with IBI322 or CD47 mAb Hu5F9 at dosing of 10 mg/kg. IBI322 was well tolerated, with less than 20% drop in RBCs and HGB counts in all monkeys (Fig. 7a, b). But in the Hu5F9 group, a substantial drop in RBC number (near 35%), hemoglobin number (near 35%), and hematocrit number (near 50%) was observed after the first dose (Fig. 7a, b, c). Compared with Hu5F9 treatment, a second dose of IBI322 led to an additional small drop in the RBC and hematocrit indices. Although RBC numbers started to recover on day 11 in both groups, IBI322 showed a significantly higher RBC count than the Hu5F9 group on day 15. We did not observe any other clinical symptoms, hematological toxicities, or macroscopic evidence of target organ toxicity attributable to the treatment. This NHP study suggested that IBI322 had lower risks of hematocrit toxicities than CD47 mAb.

Discussion

Emerging evidence has suggested that upregulation of CD47 is an important mechanism for tumor immune evasion and disease progression. Therapeutic agents targeting the CD47-SIRPα axis to modulate macrophage-mediated tumor phagocytosis have demonstrated promising anti-tumor efficacy in both preclinical and clinical studies [7, 24, 25]. Nevertheless, a major concern for systemic administration of CD47 blockade agents is the on-target/off-tumor effects given the ubiquitous expression of CD47 in normal tissues. Liu et al.

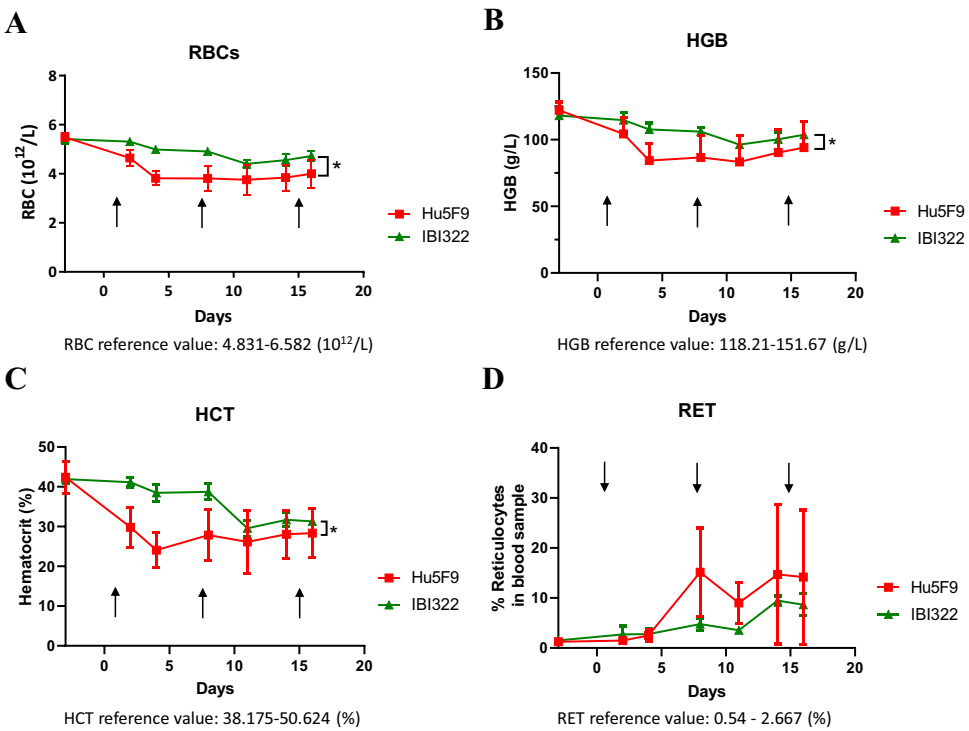

Fig. 7 NHP study with IBI322 and Hu5F9. Graphs summarize changes in RBCs (**a**), hemoglobin (**b**), hematocrit (**c**), and reticulocyte (**d**) numbers in response to treatment of IBI322 or Hu5F9 in cynomolgus monkeys. Arrows in graphs indicate antibody dosing

has postulated that using a low priming dose of hu5F9 could stimulate young RBCs production and facilitate the tolerance of subsequent high maintenance doses in NHPs [26]. Although this priming maintenance dosing approach led to mitigated anemia in most hu5F9-treated patients, about 20% of them still experienced grade 3 anemia, including 4.5% serious cases [7]. In addition, to offset "antigen sink"-mediated fast clearance and achieve sufficient serum exposure, hu5F9 was administered at a very high maintenance dose (weekly 30 mg/kg), posing a substantial treatment burden on patients.

A bispecific antibody that targets both CD47 and PD-L1 provides an innovative solution to these problems. PD-L1 is a highly expressed antigen on multiple tumors, and recent studies have demonstrated that CD47 and PD-L1, both activated by oncogenic c-Myc signaling in tumor cells, cooperatively suppressed anti-tumor immune responses [12, 27]. In addition, both PD-L1 and CD47 were co-expressed on tumor cells, whereas most normal cells (eg. RBCs) had only limited PD-L1 expression [10]. The differential co-expression pattern of CD47 and PD-L1 in tumors versus normal tissues supported the rationale of designing a bispecific antibody that could selectively recognize PD-L1-positive tumor cells and inhibit their CD47 signal to trigger phagocytosis, while sparing cells with no/low PD-L1 expression. In this present work, we described a novel "1 + 2" CD47/PD-L1 bispecific antibody IBI322 with three important features: (a) efficient tumor targeting to minimize antigen sink, (b) selective CD47 blockade on tumor rather than normal cells, and (c) dual inhibition of CD47 and PD-L1 signals to synergistically activate anti-tumor immune responses. Antigen sink issues and the effects on normal tissues were mitigated by using a monovalent anti-CD47 Fab arm in IBI322, which exhibited ~ 10–30-fold weaker binding and blocking activities than its parental CD47 antibody in PD-L1-negative cells. Tumor selectivity mediated by the anti-PD-L1 arm was achieved by using bivalent, tandem repeated high affinity PD-L1 antibody fragments. The anti-PD-L1 arm directed IBI322 binding to double-positive tumor cells, whereas the anti-CD47 arm stabilized antibody binding via the avidity effect. As a consequence, the CD47 signal blockade was restored because of co-engagement of PD-L1 on the tumor cell surface. Indeed, our in vitro phagocytosis assay performed in a mixture of tumor cells and RBCs confirmed the selective binding of IBI322 to double-positive tumor cells, even in the presence of a large CD47 sink on RBCs, which led to high tumor CD47 occupancy and effective macrophage-mediated cell killing. These findings were further supported by radioactivity-based organ biodistribution studies in hCD47 transgenic mice. The "imbalanced affinity" design of IBI322 has led to significantly increased uptake in PD-L1-positive tumors with decreased distribution in blood depot organs compared with the parental CD47 antibody, indicating a shifted preference of tissue binding and decreased effects on peripheral antigen sinks. Furthermore, a toxicology study in NHPs revealed favorable safety profiles of IBI322 at therapeutic doses, with much milder adverse effects on RBCs than in-house generated hu5F9. As IBI322 cross-reacts with cyno PD-L1 and CD47 at similar affinities to human receptors, it is reasonable to anticipate that IBI322 would render low CD47 target-mediated adverse effects in humans. This speculation still remains to be examined in future clinical studies.

Co-targeting CD47 and PD-L1, bispecific molecule IBI322 was designed to stimulate both CD47 and PD-L1 pathways for potential synergistic anti-tumor effects. Indeed, we did observe that the bispecific molecule was more efficacious than the simple combination of anti-CD47 and anti-PD-L1 at equal molarity. We postulate that the better efficacy could be attributed to tumor-directing functionality created by the bispecific antibody. The presence of PD-L1 in Raji-hPD-L1 or A375 cells facilitated higher tumor uptake of IBI322, then locally increased drug exposure resulted in better anti-tumor effects.

In addition to co-blocking and PD-L1-dependent tumor enrichment, another mechanism of great importance is that IBI322 molecule can potentially bridge innate DC activation and T cell priming. Unfortunately, the PBMC-humanized NOD-SCID mice used in this study lacked DCs, making it difficult to evaluate this function. In that respect, a better model would be syngeneic tumors transplanted in human CD47/PD-L1 double knock-in mice. However such mice were not available at the time of this study. In addition, given the recently elucidated function of PD1 in macrophage phagocytosis [19], it would be interesting to examine whether IBI322 could show synergistic activities for both innate and adaptive immunity levels in preclinical models that fully represented human immune systems.

In conclusion, our study described a novel strategy for designing a CD47 and PD-L1 dual-blockade bispecific antibody, IBI322, which selectively targeted tumor cells while minimizing on-target toxicities in normal tissues. By harnessing both innate and adaptive immune responses, IBI322 provides an opportunity for improved cancer immunotherapy with a higher therapeutic index than the combination of anti-CD47 and anti-PD-L1 antibodies. Currently, IBI322 is in a phase 1 dose escalation trial (NCT04328831). Further clinical studies are expected to fully validate its safety and effectiveness in human patients.

Author contributions YW, HN, SZ, BC, MY, LM and JL designed the study; HN, YG, SZ, WW and ZW performed the in vitro experiment; WW, MW, YZ, BC, YW, DP, CH, ML, and YB performed the in vivo experiment and biodistribution; XQ performed the experiment in primate. HN, SZ, KH and JL wrote the manuscript. All authors read and approved the final manuscript.

Funding This work was financially supported by the National Significant New Drugs Creation Program (2017ZX09304021), Jiangsu Provincial Medical Innovation Team (CXTDA2017024), and Leading technology foundation research project of Jiangsu province (BK20192005).

Compliance with ethical standards

Conflict of interest Haiqing Ni, Shuaixiang Zhou, Kaijie He, Yarong Gao, Weiwei Wu, Min Wu, Zhihai Wu, Xuan Qiu, ying Zhou, Bingliang Chen, and Junjian Liu are employees of Innovent Biologics (Suzhou). All the remaining authors have declared no conflicts of interest.

Ethical approval All mice experiments were performed in accordance with the regulations for care and use of laboratory animals at Innovent Biologics and were approved by Innovent's Institutional Animal Care and Use Committee (IACUC-01). All monkey experiments were approved by IACUC and performed according to the regulation of AAALAC.

Animal source NOS-SCID mice and NOG mice were purchased from Beijing Vital River Laboratory Animal Technology Co., Ltd. (Beijing, China). Human CD47 knock-in mice were purchased from Biocytogen, Inc. (Beijing, China). Cynomolgus monkeys were purchased from Beijing Prima Biotech Inc.

Cell line authentication RAJI, A375, CCRF-CEM, and H292 cell lines were obtained from ATCC (Manassas, VA). CHO-S cell line was obtained from Themo Fisher Scientific, Carlsbad, CA, USA). MC38 cell line was obtained from Shanghai Model Organisms Center, Inc. (Shanghai, China). PBMC cells were purchased from Allcells (Alameda, CA, USA).

References

1. Brown EJ, Frazier WA (2001) Integrin-associated protein (CD47) and its ligands. Trends Cell Biol 11(3):130–135. https://doi.org/10.1016/S0962-8924(00)01906-1
2. Barclay AN, Berg TKVD (2014) The interaction between signal regulatory protein alpha (SIRPα) and CD47: structure, function, and therapeutic target. Annu Rev Immunol 32(1):25–50. https://doi.org/10.1146/annurev-immunol-032713-120142
3. Majeti R, Chao MP, Alizadeh AA, Pang WW, Jaiswal S, Gibbs KD Jr, van Rooijen N, Weissman IL (2009) CD47 is an adverse prognostic factor and therapeutic antibody target on human acute myeloid leukemia stem cells. Cell 138(2):286–299. https://doi.org/10.1016/j.cell.2009.05.045
4. Jaiswal S, Jamieson CHM, Pang WW, Park CY, Chao MP, Majeti R, Traver D, van Rooijen N, Weissman IL (2009) CD47 is upregulated on circulating hematopoietic stem cells and leukemia cells to avoid phagocytosis. Cell 138(2):271–285. https://doi.org/10.1016/j.cell.2009.05.046
5. Chao MP, Alizadeh AA, Tang C, Myklebust JH, Varghese B, Gill S, Jan M, Cha AC, Chan CK, Tan BT, Park CY, Zhao F, Kohrt HE, Malumbres R, Briones J, Gascoyne RD, Lossos IS, Levy R, Weissman IL, Majeti R (2010) Anti-CD47 antibody synergizes with rituximab to promote phagocytosis and eradicate non-hodgkin lymphoma. Cell 142(5):699–713. https://doi.org/10.1016/j.cell.2010.07.044
6. Willingham SB, Volkmer J-P, Gentles AJ, Sahoo D, Dalerba P, Mitra SS, Wang J, Contreras-Trujillo H, Martin R, Cohen JD, Lovelace P, Scheeren FA, Chao MP, Weiskopf K, Tang C, Volkmer AK, Naik TJ, Storm TA, Mosley AR, Edris B, Schmid SM, Sun CK, Chua M-S, Murillo O, Rajendran P, Cha AC, Chin RK, Kim D, Adorno M, Raveh T, Tseng D, Jaiswal S, Enger PØ, Steinberg GK, Li G, So SK, Majeti R, Harsh GR, van de Rijn M, Teng NNH, Sunwoo JB, Alizadeh AA, Clarke MF, Weissman IL (2012) The CD47-signal regulatory protein alpha (SIRPa) interaction is a therapeutic target for human solid tumors. Proc Natl Acad Sci 109(17):6662–6667. https://doi.org/10.1073/pnas.1121623109
7. Advani R, Flinn I, Popplewell L, Forero A, Bartlett NL, Ghosh N, Kline J, Roschewski M, LaCasce A, Collins GP, Tran T, Lynn J, Chen JY, Volkmer J-P, Agoram B, Huang J, Majeti R, Weissman IL, Takimoto CH, Chao MP, Smith SM (2018) CD47 blockade by Hu5F9-G4 and rituximab in non-Hodgkin's lymphoma. N Engl J Med 379(18):1711–1721. https://doi.org/10.1056/NEJMoa1807315
8. Sallman DA, Donnellan WB, Asch AS, Lee DJ, Malki MA, Marcucci G, Pollyea DA, Kambhampati S, Komrokji RS, Elk JV, Lin M, Agoram B, Chen JY, Volkmer J-P, Takimoto CHM, Chao M, Vyas P (2019) The first-in-class anti-CD47 antibody Hu5F9-G4 is active and well tolerated alone or with azacitidine in AML and MDS patients: initial phase 1b results. J Clin Oncol 37:7009–7009. https://doi.org/10.1200/JCO.2019.37.15_suppl.7009
9. Sikic BI, Lakhani N, Patnaik A, Shah SA, Chandana SR, Rasco D, Colevas AD, O'Rourke T, Narayanan S, Papadopoulos K, Fisher GA, Villalobos V, Prohaska SS, Howard M, Beeram M, Chao MP, Agoram B, Chen JY, Huang J, Axt M, Liu J, Volkmer J-P, Majeti R, Weissman IL, Takimoto CH, Supan D, Wakelee HA, Aoki R, Pegram MD, Padda SK (2019) First-in-human, first-in-class phase I trial of the anti-cd47 antibody Hu5F9-G4 in patients with advanced cancers. J Clin Oncol 37(12):946–953. https://doi.org/10.1200/jco.18.02018
10. Liu B, Guo H, Xu J, Qin T, Guo Q, Gu N, Zhang D, Qian W, Dai J, Hou S, Wang H, Guo Y (2018) Elimination of tumor by CD47/PD-L1 dual-targeting fusion protein that engages innate and adaptive immune responses. m Abs 10(2):315–324. https://doi.org/10.1080/19420862.2017.1409319
11. Lian S, Xie R, Ye Y, Lu Y, Cheng Y, Xie X, Li S, Jia L (2019) Dual blockage of both PD-L1 and CD47 enhances immunotherapy against circulating tumor cells. Sci Rep 9(1):4532. https://doi.org/10.1038/s41598-019-40241-1
12. Liu X, Liu L, Ren Z, Yang K, Xu H, Luan Y, Fu K, Guo J, Peng H, Zhu M, Fu Y-X (2018) Dual targeting of innate and adaptive checkpoints on tumor cells limits immune evasion. Cell Rep 24(8):2101–2111. https://doi.org/10.1016/j.celrep.2018.07.062
13. Chen L, Han X (2015) Anti–PD-1/PD-L1 therapy of human cancer: past, present, and future. J Clin Investig 125(9):3384–3391. https://doi.org/10.1172/JCI80011
14. Sanmamed MF, Chen L (2018) A paradigm shift in cancer immunotherapy: from enhancement to normalization. Cell 175(2):313–326. https://doi.org/10.1016/j.cell.2018.09.035
15. Brahmer JR, Tykodi SS, Chow LQM, Hwu W-J, Topalian SL, Hwu P, Drake CG, Camacho LH, Kauh J, Odunsi K, Pitot HC, Hamid O, Bhatia S, Martins R, Eaton K, Chen S, Salay TM, Alaparthy S, Grosso JF, Korman AJ, Parker SM, Agrawal S, Goldberg SM, Pardoll DM, Gupta A, Wigginton JM (2012) Safety and activity of anti–PD-L1 antibody in patients with advanced cancer. N Engl J Med 366(26):2455–2465. https://doi.org/10.1056/NEJMoa1200694
16. Wilky BA (2019) Immune checkpoint inhibitors: The linchpins of modern immunotherapy. Immunol Rev 290(1):6–23. https://doi.org/10.1111/imr.12766
17. Topalian SL, Hodi FS, Brahmer JR, Gettinger SN, Smith DC, McDermott DF, Powderly JD, Carvajal RD, Sosman JA, Atkins MB, Leming PD, Spigel DR, Antonia SJ, Horn L, Drake CG, Pardoll DM, Chen L, Sharfman WH, Anders RA, Taube JM,

McMiller TL, Xu H, Korman AJ, Jure-Kunkel M, Agrawal S, McDonald D, Kollia GD, Gupta A, Wigginton JM, Sznol M (2012) Safety, activity, and immune correlates of Anti–PD-1 antibody in cancer. N Engl J Med 366(26):2443–2454. https://doi.org/10.1056/NEJMoa1200690

18. Brahmer JR, Drake CG, Wollner I, Powderly JD, Picus J, Sharfman WH, Stankevich E, Pons A, Salay TM, McMiller TL, Gilson MM, Wang C, Selby M, Taube JM, Anders R, Chen L, Korman AJ, Pardoll DM, Lowy I, Topalian SL (2010) Phase I study of single-agent anti-programmed death-1 (MDX-1106) in refractory solid tumors: safety, clinical activity, pharmacodynamics, and immunologic correlates. J Clin Oncol 28(19):3167–3175. https://doi.org/10.1200/jco.2009.26.7609
19. Gordon SR, Maute RL, Dulken BW, Hutter G, George BM, McCracken MN, Gupta R, Tsai JM, Sinha R, Corey D, Ring AM, Connolly AJ, Weissman IL (2017) PD-1 expression by tumour-associated macrophages inhibits phagocytosis and tumour immunity. Nature 545(7655):495–499. https://doi.org/10.1038/nature22396
20. Merchant AM, Zhu Z, Yuan JQ, Goddard A, Adams CW, Presta LG, Carter P (1998) An efficient route to human bispecific IgG. Nat Biotechnol 16(7):677–681. https://doi.org/10.1038/nbt0798-677
21. Wang J, Fei K, Jing H, Wu Z, Wu W, Zhou S, Ni H, Chen B, Xiong Y, Liu Y, Peng B, Yu D, Jiang H, Liu J (2019) Durable blockade of PD-1 signaling links preclinical efficacy of sintilimab to its clinical benefit. Am Abs 11(8):1443–1451. https://doi.org/10.1080/19420862.2019.1654303
22. England CG, Ehlerding EB, Hernandez R, Rekoske BT, Graves SA, Sun H, Liu G, McNeel DG, Barnhart TE, Cai W (2017) Preclinical pharmacokinetics and biodistribution studies of 89Zr-labeled pembrolizumab. J Nucl Med 58(1):162–168. https://doi.org/10.2967/jnumed.116.177857
23. Tavare R, Escuin-Ordinas H, Mok S, McCracken MN, Zettlitz KA, Salazar FB, Witte ON, Ribas A, Wu AM (2016) An effective immuno-PET imaging method to monitor CD8-dependent responses to immunotherapy. Cancer Res 76(1):73–82. https://doi.org/10.1158/0008-5472.CAN-15-1707
24. Chao MP, Majeti R, Weissman IL (2012) Programmed cell removal: a new obstacle in the road to developing cancer. Nat Rev Cancer 12(1):58–67. https://doi.org/10.1038/nrc3171
25. Wu L, Yu G-T, Deng W-W, Mao L, Yang L-L, Ma S-R, Bu L-L, Kulkarni AB, Zhang W-F, Zhang L, Sun Z-J (2018) Anti-CD47 treatment enhances anti-tumor T-cell immunity and improves immunosuppressive environment in head and neck squamous cell carcinoma. OncoImmunology 7(4):e1397248. https://doi.org/10.1080/2162402X.2017.1397248
26. Liu J, Wang L, Zhao F, Tseng S, Narayanan C, Shura L, Willingham S, Howard M, Prohaska S, Volkmer J, Chao M, Weissman IL, Majeti R (2015) Pre-clinical development of a humanized anti-CD47 antibody with anti-cancer therapeutic potential. PLoS ONE 10(9):e0137345. https://doi.org/10.1371/journal.pone.0137345
27. Casey SC, Tong L, Li Y, Do R, Walz S, Fitzgerald KN, Gouw AM, Baylot V, Gütgemann I, Eilers M, Felsher DW (2016) MYC regulates the antitumor immune response through CD47 and PD-L1. Science 352(6282):227–231. https://doi.org/10.1126/science.aac9935